Research Article

CHO Cell Cultures in Shake Flasks and Bioreactors present different Host Cell Protein Profiles in the supernatant

Cher H Goey[1]

David Bell[2]

Cleo Kontoravdi[1]

[1]Department of Chemical Engineering, Centre for Process Systems Engineering, Imperial College London, London, U.K.

[2]Department of Medicine, Imperial College London, London, U.K.

Correspondence: Dr. Cleo Kontoravdi, Department of Chemical Engineering, Centre for Process Systems Engineering, Imperial College London, South Kensington Campus, SW7 2AZ, London, U.K.

E-mail: cleo.kontoravdi@imperial.ac.uk

Keywords:

Apoptosis, bioreactor, cell cycle distribution, Chinese hamster ovary, host cell protein, mild hypothermia

Abbreviations:

CHO, Chinese hamster ovary; **HCP,** host cell protein; **IVCC,** integrated viable cell concentration; **mAb,** monoclonal antibody; **QbD,** Quality by design; **TDS,** temperature downshift; **VCD,** viable cell density; **vvm,** gas volume flow per unit of liquid volume per minute;

Abstract

Several studies on the impact of cell culture parameters on the profile of host cell protein (HCP) impurities have been carried out in shake flasks. Herein, we explore how transferable the findings and conclusions of such investigations are to lab-scale bioreactors. Experiments were performed in both systems in fed-batch mode under physiological temperature and with a shift to mild hypothermia and the impact on key upstream performance indicators was quantified. Under both temperatures, bioreactors produced a richer HCP pool despite the overall concentration being similar in both scales and temperatures. The number of different HCPs detected in bioreactor supernatants was four times higher than that in flasks under physiological temperature and more than eight times higher under mild hypothermia. The origin of HCPs was also altered from mostly naturally secreted proteins in flasks to mainly intracellular proteins in bioreactors at the lower temperature. Although the number of species correlated with apoptotic cell density in bioreactors, this was not the case in flasks. Even though the level of HCP impurities and mAb/HCP concentration ratio were similar under all four conditions with an average of approximately 330 μg HCP/mL culture and 0.3 mg HCP/mg IgG4, respectively, the fact that culture method significantly affects the number of species present in the supernatant can have implications for downstream processing steps.

Highlights

1. Comparison of flask and bioreactor cultures at 37°C and 32°C
2. All four conditions produced similar HCP concentration and mAb/HCP ratio
3. Bioreactor cultures had significantly higher number of HCP species than flasks
4. HCP variety correlated with apoptotic cell density in bioreactors but not flasks

1 Introduction

Removal of HCPs has been a significant challenge in the biopharmaceutical industry as downstream purification (DSP) reaches its capacity bottleneck [1]. Subsets of HCPs that cannot be easily removed by the Protein A chromatography step, which is the workhorse of monoclonal antibody (mAb) platform purification processes, have been extensively identified [2-7]. Furthermore, HCPs such as chaperones and proteases may compromise product quality by promoting product aggregation or fragmentation [8-10]. In the past five years, the concept of Quality by Design (QbD) had been employed to understand the impact of upstream culture conditions like cell age, cell culture mode (batch or fed-batch), process duration and culture temperature on HCP profile [11-14] with an aim to reduce the level of HCPs in downstream feedstock by optimizing cell culture conditions.

Several of these studies were carried out in flasks [4,11], while others performed research with bioreactors that mimic typical biopharmaceutical productions [13-15]. However, our understanding of how different culture methods in flasks versus bioreactors affect the extracellular HCP profile at harvest is limited. As we try to integrate findings from a variety of experimental studies ranging from characterizing extracellular HCP profile to mapping intracellular metabolic pathways, it becomes essential to understand how cells behave under different culture environments and whether information obtained from flask cultures [4,16-19] still holds true when we scale cultures up to lab-scale bioreactors and beyond. For example, does scale-up from flasks to bioreactors change the dynamics between cellular behavior and the corresponding HCP profile? We recently reported that the HCP level in supernatant collected from bioreactors increases proportionally with the percentage of dead cells, while the degree of apoptosis determines the variety of HCP species found in the supernatant [13]. Would these correlations have been identified had the study been conducted in shake flasks?

In this work, we investigate the impact of scale-up from flasks to lab-scale bioreactors on CHO cell behavior and the corresponding extracellular HCP concentration and variety at harvest. First, we characterize the impact of cell culture methods (flasks or bioreactors) on a set of CHO cell responses including cell growth, cell health, and cell cycle distribution under standard physiological temperature and with a shift to mild hypothermia during exponential cell growth phase. Then, proteomic analysis of supernatants collected at the harvest criterion of 80% culture viability is conducted and the HCP species present under the different culture methods are categorized. Finally, interlinks between cellular behavior and HCP profile are identified and related to the culture environment encountered by the cells in flasks and bioreactors, highlighting key differences that can result in significantly different predictors of HCP variety at each scale.

2 Materials and methods

2.1 Cell line and maintenance

GS-CHO 46 cell line expressing glutamine synthetase and cB72.3 chimeric IgG_4 antibody was kindly donated by Lonza Biologics. The cell line was revived and cultured in shake flasks (Corning, NY) in CD CHO medium (Life Technologies, Paisley, UK) at 37°C in 8% CO_2 humidified air, shaken at 140 rpm. Cells were subcultured in fresh medium every four days at a seeding density of 2 x 10^5 cells/mL and then used to seed shake flask and bioreactor fed-batch cultures on the fourth passage. The first and second passages were supplemented with 25 μM L-Methionine Sulfoximine (MSX, Sigma-Aldrich, Dorset, UK).

2.2 Shake flask cell culture

Shake flask cultures were performed in triplicate in 500 mL Erlenmeyer flasks (Corning, NY) with a working volume of 130 mL in CD CHO medium. Cell cultures were seeded at a cell density of 2 x 10^5 viable cells/mL and grown in 8% CO_2 humidified air, shaking at 140 rpm. For the control experiment, the culture temperature was maintained at 37°C, whereas a second set of triplicate cultures were grown at 37°C until late exponential growth phase (day 5), when the temperature was down-shifted to 32°C and maintained until harvest.

All cultures were supplemented with 10% v/v CD EfficientFeed™ C AGT™ (Feed-C, Life Technologies, Paisley, UK) every other day from day 2. Every day, a 5 mL culture sample was removed and centrifuged at 800 rpm for 5 min to obtain the supernatant, which was then aliquoted and stored at -80°C. All cultures were harvested when viability dropped below 80%.

2.3 Bioreactor operation

The 3L CellReady bioreactor (Applikon Biotechnology, Schiedam, Netherlands) was inoculated at a seeding density of 3 x 10^5 cells/mL with an initial cell culture volume of 1.2 L. The culture was mixed by an in-house up-pumping marine impeller rotating at 150 rpm and was supplied with a constant air flow rate of 22.5 mL/min. The process was controlled with a my-control unit (Applikon Biotechnology, Schiedam, Netherlands) at 36.5 ± 0.5°C with a heating blanket and pH 7.0 ± 0.1 with CO_2 supply and 100 mM $NaHCO_3$/Na_2CO_3 alkali solution (Sigma-Aldrich, Dorset, UK). Dissolved oxygen tension (DOT) was set to a minimum of 50% with oxygen supply. These process parameters were monitored continuously with the BioExpert software version 1.1X (Applikon Technology, Schiedam, Netherlands).

Cell cultures were supplemented with 10% v/v CD EfficientFeed™ C AGT™ (Feed-C, Life Technologies, Paisley, UK) on alternate days from day 2. Foaming was relieved with 5 mL of 5% w/v Antifoam-C (Sigma-Aldrich, Dorset, UK). Samples were collected daily and centrifuged at 800 rpm for 5 min. Aliquoted supernatants were stored at -80°C. The bioreactor working volume was kept within the range of 1-1.3 L by drawing out excessive culture fluid every day after sampling and before any addition of feed or antifoam. For mild hypothermic experiments, cell culture temperature was reduced to 32.0 ± 0.5°C on day 5, corresponding to the late exponential cell growth phase, and maintained constant until harvest. Two bioreactor runs were conducted under each temperature regime.

2.4 Cell count, cell cycle distribution and cell health

Cell concentration was determined with the Viability and Cell Count assay of the NucleoCounter® NC-250™ (ChemoMetec A/S, Allerod, Denmark) according to the manufacturer's instructions. Total DNA content and cell cycle distribution were determined with the 2-Step Cell Cycle assay of the NucleoCounter® NC-250™, and the results were visualized and analyzed with the associated NucleoView software. Examination of cellular health was carried out with the Vitality assay of the NucleoCounter® NC-250™. All solutions (Solution 18 for the Cell count assay, Solutions 10, 11 and 12 for the 2-Step Cell cycle assay and Solution 6 for the Vitality assay) were purchased from ChemoMetec A/S (Allerod, Denmark).

2.5 Measurements of extracellular IgG_4 and metabolite concentrations

Extracellular IgG_4 concentration was measured with the BLItz system (Pall ForteBio Europe, Portsmouth, UK), which is a biolayer interferometry device. Extracellular concentrations of glucose (Glc), glutamate (Glu), glutamine (Gln), lactate (Lac) and ammonia (Amm) were quantified with the BioProfile 400 analyzer (NOVA Biomedical, MA, USA).

2.6 Quantification of HCP concentration and identification of HCP species

HCP concentration in the cell culture supernatant was measured with a commercially available GS-HCP ELISA assay kit (Lonza Biologics, Slough, UK). HCP species in the culture supernatant were detected with liquid chromatography-mass spectrometry/mass spectrometry (LC-MS/MS). The protocol for sample preparation was adapted from the method described by Reisinger et al. (2014). Samples were filtered with 0.45μm syringe filters (VWR, Darmstadt, Germany). Total protein concentration of the filtered supernatant was measured with NanoDrop 1000 (Thermo Scientific, UK). Then, 450μg of total protein were denatured in 4 M guanidine HCl (Sigma-Aldrich, Dorset, UK) and reduced with 6.4mM dithiothreitol, DTT (Sigma-Aldrich, Dorset, UK) at 37°C for 1 hour. The sample was then alkylated with 13mM iodoacetamide (Sigma-Aldrich, Dorset, UK) in the dark at room temperature (around 20°C) for 1 hour. After that, the sample was quenched by adding 4.2 mM DTT and buffer exchanged to 50mM, pH 8.0 Tris (Sigma-Aldrich, Dorset, UK) with 10K Microcon centrifugal filter devices (Merck Millipore, Cork, Ireland). MS-grade trypsin (Promega, WI, USA) was added with a mass ratio of 1μg of trypsin to 22μg of protein and left overnight at 37°C. Prepared samples were aliquoted and stored at -80°C until analysis.

Trypsin digested samples were analysed with an Infinity 1290 Binary LC system coupled to an iFunnel 6550 Quadrupole-Time-of-Flight liquid chromatography-mass spectrometer, QTOF LC-MS (Agilent Technologies, Santa Clara, CA). 20 μL of the tryptic peptide sample was separated on a Zorbax Extend-C18 LC column, with 2.1 x 50mm dimensions and 1.8μm particle size (Agilent Technologies, Santa Clara, CA) by an 80-minute gradient (solvent A: 0.1% formic acid in water; solvent B: 0.1% formic acid in acetonitrile). The following linear gradient was applied: 3-40% buffer

B for 80 min, 40-90% buffer B over 2 min then 100% buffer B over 2 min. Peptides were subjected to mass spectrometry (MS) and MS/MS as they eluted from the LC.

The data files acquired were extracted to generate peak lists, then submitted for database searches through the Spectrum Mill MS proteomic workbench, Rev B04.01.141 (Agilent Technologies, Santa Clara, CA). The spectra were searched against an in-house database of protein sequences of rodents (reviewed proteins of Cricetulus griseus, Mesocricetus auratus, Mus musculus and Rattus norvegicus downloaded from the UniProt website on 10-4-2015), IgG_4, and common contaminants like human keratins. Proteins identified with 95% confidence or greater were accepted.

2.7 HCP categorization

HCPs in the supernatants of shake flasks and bioreactors were categorized further into three main subcellular locations according to the information available on the UniProt website (http://www.uniprot.org): intracellular, cell plasma membrane and naturally secreted. Intracellular HCPs include proteins that could only be found in the supernatant if cells lyse, which include proteins located in the cytoplasm, nucleus, endoplasmic reticulum (ER), Golgi apparatus, mitochondrion, ribosomal units, cytoplasmic vesicles, storage granules and structural membrane proteins of the intracellular organelles. Cell membrane HCPs include structural proteins that form the cell plasma membrane, proteins on cell surface, microvillus and proteins at cell-cell junctions. Secreted HCPs include proteins in extracellular matrix and those excreted through exosomes. HCPs that were found in more than one location according to the UniProt website, e.g., being modified in the ER and Golgi to be secreted, the HCPs would be categorized according to its final destination as a secreted protein.

3 Results and Discussion

3.1 Cell growth

Figure 1 shows the cell growth profiles of cultures in flasks and bioreactors at (A) standard physiological temperature and (B) under mild hypothermia. Cells cultured in bioreactors reached a maximum cell density of 1.5×10^7 cells/mL, which was 60% higher than that of flask cultures. On day 14, the IVCC was 30% higher in bioreactors than in flasks. However, it should be mentioned that the bioreactors were seeded at 3×10^5 cells/mL instead of 2×10^5 cells/mL in flasks, although it is evident from Figure 1 that this did not impact the initial cell growth rate and in the case of mild hypothermic cultures did not result in any significant difference in the profile of viable cell density. A fluctuating stationary phase was observed in the control bioreactor experiment from day 7 to 10 in contrast to a smooth and stable stationary profile in flask cultures (
Figure 1A). We believe that feeding at 10% culture volume every alternate day was the cause of this. Cell culture fluid was drawn out before feeding to maintain a working volume of 1-1.3 L, which, in combination with the feeding events, diluted

the cultures slightly. In contrast to the control, cell cultures conducted under mild hypothermia produced similar growth curves in both flasks and bioreactors (

Figure 1B). The exponential cell growth of both bioreactors and flasks was ceased immediately upon TDS on day 5, and an extended stationary phase commenced from day 6. Cell growth was not enhanced by the controlled environment in bioreactors. In both culture methods, the extracellular ammonia concentration was lower under physiological temperature, while it exceeded the threshold for growth-inhibitory levels, reported to be 5mM for this cell line [20], under mild hypothermia from day 6 in flasks and from day 7 in bioreactors (data not shown). This is expected to have contributed to the lower IVCC under mild hypothermia.

At standard physiological temperature, cell viability of bioreactors could not be sustained although the IVCC and maximum cell density were increased significantly compared to flasks (

Figure 1A). Cell viability dropped below 90% at the start of the stationary phase (day 8). In contrast, culture viability in flasks was maintained at a high level and only decreased in late stage culture. On day 14, cell viability of the control flasks and bioreactors were 84.1 ± 4.1% and 48.5 ± 8.0%, respectively. TDS improved cell viability of bioreactors significantly, which was maintained at a similar level as that of flask cultures and began to decrease only from day 11 onwards (

Figure 1B).

We wanted to identify the reasons for this rapid decline and, therefore, analyzed the extracellular metabolite profiles, CO_2 accumulation, working volume and stirring speed of the bioreactors and compared them to data available in the literature. The extracellular glucose concentration, which is the main carbon source for the cultures, was above the minimum threshold of 2 g/L (or 11 mmol/L, Figure S5A). Lactate level was also within an acceptable range for healthy cell cultures despite the continuous accumulation, peaking well under 3 g/L (Figure S5B). Zhu et al. reported that osmolarity above 460 mmol/L is detrimental to CHO cell viability and growth [21]. Nonetheless, the osmolarity of the control bioreactors was below 420 mmol/L on day 8 when cell viability dropped below 90%. Equally, CO_2 was stripped off with a constant air flow rate of 0.02 vvm from the start of the process, and oxygen was supplied through an air-oxygen cascade from day 6 onwards when dissolved oxygen started to be on demand. Nonetheless, we are unsure if sufficient CO_2 stripping was achieved particularly at the late exponential phase when cell density increased above 1.5×10^7 cells/mL, since the partial pressure of CO_2 was not monitored on-line.

However, Odeleye et al. studied the fluid dynamics of the 3L CellReady disposable bioreactor system and demonstrated that the well-mixed region of the bioreactor is limited up to a z/H = 0.15 (level of the culture/ height of the bioreactor) [22]. The region extending from z/H of 0.2 to the liquid surface was characterized as a low energy region where mass, heat and gas transfers were heterogeneous. We therefore kept the working volume of the bioreactor in 1.2-1.3 L to maintain culture homogeneity. Nonetheless, cell culture at smaller volumes also suggests that cells

would circulate the blade area at higher frequencies. As reported by Odeleye et al., the lower circulation loop exhibits higher turbulence levels and the greater hydrodynamic forces could damage the cells as studied by Godoy-Silva et al. [23]. Therefore, we hypothesize that the early cell death in the control experiments was caused by cells experiencing significant hydrodynamic forces around the blade area of the bioreactors.

This conclusion is also supported by Velez-Suberbie et al. who cultured a similar CHO cell line expressing IgG_4 in 3.5 L bioreactors at 37°C [24]. The bioreactors were aerated by direct gas sparging, and the results showed that cell viability dropped below 30% within 24 hours after inoculation in the absence of shear protectant. In contrast, bioreactors supplemented with a shear protectant, Pluronic F-68, were successful. Velez-Suberbie et al. concluded that cells could not survive with direct gas sparging without the addition of shear protectant. Similar conclusions were made by Clincke et al. and Zhang et al. regarding the importance of shear protectants on sustaining cell viability of bioreactors [25,26].

Interestingly, cell viability was maintained at high percentages in mild hypothermic bioreactors operated in similar working volume, stirring speed and aeration rate as the control. Cells at 32°C appeared to be more robust than the control which is believed to be a result of homeoviscous adaptation of the cell membrane at lower culture temperature [12,13,27].

3.2 Cell health and cell cycle distribution

Cell health of flasks and bioreactors was measured with the Vitality assay of NucleoCounter-250, and the results of cell cultures at standard physiological temperature and mild hypothermia are shown in **Figure 2**A and B, respectively. Under all culture conditions and methods, over 90% of cells were healthy with apoptotic subpopulation below 2% in the first six days. At standard physiological temperature, the apoptotic subpopulation of both flasks and bioreactors started to rise from day 7 (**Figure 2**A). Interestingly, the percentage of apoptotic cells increased at a higher rate in flasks than in bioreactors. From day 13 onwards, the percentage of apoptotic cells accumulated to approximately 10% of total cells in flasks, which is double of that in bioreactors (**Figure 2**A). Mild hypothermic cultures showed similar cell health trend as that of the controls, where the percentage of apoptotic cells increased significantly in flasks but remained at lower levels in the corresponding bioreactors (**Figure 2**B). Accumulation of apoptotic cells across the cell culture period are shown in Figure S1 and S2.

Figure 2C and D show the cell cycle distribution of flasks and bioreactors at standard physiological temperature and under mild hypothermia, respectively. Cell cultures with flasks had active cell divisions through the exponential phase with a low percentage of G_0/G_1 subpopulation of 62.2 ± 0.5% and high S and M subpopulations of a total 33.0 ± 0.5% cells (**Figure 2**C). After six days, the fraction of

cells in G_0/G_1 increased gradually and reached 80.4 ± 0.4% of cells arrested in G_0/G_1 on day 10 (**Figure 2**C). Scale-up from shake flask to bioreactor at standard physiological temperature changed the cell cycle distribution of the culture. Distinct patterns of cell cycle distribution across the culture period were not observed (**Figure 2**C): G_0/G_1 subpopulation increased gradually during the exponential phase for six days, after which the control bioreactor duplicate started to behave differently, as reported in our previous study [13]. The G_0/G_1 subpopulation increased continuously until harvest in one but decreased continuously in another. The decrease in G_0/G_1 cells in the latter case was accompanied by an increase in apoptotic cell population with fragmented DNA [28,29].

Both flask and bioreactor cultures responded to TDS immediately with a rise in G_0/G_1 subpopulation from 66.9 ± 0.5% on day 5 to 80.9 ± 1.1% on day 6 (**Figure 2**D). Interestingly, cell cycle arrest in flasks was temporary. The percentage of cells in G_0/G_1 returned to a lower value of 72.2 ± 0.2% after an adaptation period of seven days on day 13 and remained stable through the late stationary and decline phases. In contrast, cell cycle arrest in the mild hypothermic bioreactors was permanent, where G_0/G_1 cells remained at high percentages of over 77% until the end of the cultures. Active cell division was not resumed, which resulted in a lower VCD in the decline phase (

Figure 1B). The cause of different cell cycle responses to TDS in bioreactors and flasks is yet to be investigated. A possible reason for permanent cell arrest in bioreactors was the higher hydrodynamic stress experienced by cells in such an environment. This is supported by Motobu et al. who showed that CHO cells exposed to great hydrodynamic force have an increased fraction of G_0/G_1 cells [30]. In contrast, static cell culture retains fewer cells in G_0/G_1 phase but more cells in S phase.

Cells cultured in shake flasks exhibited a larger apoptotic subpopulation than bioreactors regardless of the culture temperature (**Figure 2**). We propose two reasons for this observation. Firstly, critical cell culture parameters like pH and dissolved oxygen were not controlled in flasks. Moreover, daily sampling required flasks to be taken out from the incubators when the temperature of the cultures would have been perturbed. Fluctuations in these important process parameters in flasks can impose stresses onto the cultures, and, hence, prevent cells from growing as healthily as that in the fully controlled bioreactors.

The second reason is that apoptotic cells, which are more fragile and shear-sensitive than healthy cells, were quickly broken down to cell debris in the high-shear bioreactor environment [12]. Therefore, accumulation of apoptotic cells over the culture timeframe was not observed. The second reason is also supported by the fact that the percentage of dead cells in bioreactors increased continuously although the apoptotic cell population remained low (

Figure 1A). Additionally, we found a subpopulation of cells with PI intensity higher than the main healthy cell population in bioreactors from mid-stationary phase onwards (Figure S1G to L). This subpopulation of cells increased with the culture duration especially in the control bioreactors but did not exist in flasks at

both culture temperatures (Figure S1A to F and Figure S2A to F). Examination of cell images revealed that this cell population arose from aggregations of viable cells in bioreactors. These aggregates consisted of several viable cells with one or two dead cells or cell debris scattered among them. The presence of dead cells interfered with the overall PI intensity of the viable aggregates, hence, deviated their locations on the scatter plots.

3.3 IgG_4 and HCP concentrations

Figure 3A and B show the IgG_4 titer of flask and bioreactor cultures at standard physiological temperature and under mild hypothermia. Production of IgG_4 was higher in bioreactors than flasks under both temperatures (**Figure 3**A and B), which is also reflected in the higher specific cell productivity, Q_P (**Table 1**). **Figure 3**C and D show the extracellular HCP concentration in flasks and bioreactors at standard physiological temperature and under mild hypothermia, respectively. Accumulation of HCPs was observed in all four cases, but the HCP concentration was always lower in flasks than in the corresponding bioreactors. The extracellular HCP level of the control flasks increased significantly by 2.2-fold in mid-stationary phase (from day 8 to 10, **Figure 3**C), when cell viability was still very high (95.2 ± 1.3%). On the other hand, control bioreactors produced a large quantity of HCPs from the beginning of stationary phase exceeding 200 μg/mL on day 7 and accumulating continuously until harvest. The step-increase in HCP level was postponed from mid- to late stationary phase when cells were cultured in flasks under mild hypothermia (from day 12 to 14). Similar to the control, this happened when cell viability was still high (94.6 ± 1.4%, on day 14). The mean HCP concentration of bioreactors under mild hypothermia was higher than that of the corresponding flasks at harvest, but the difference was not statistically significant (272.0±75.3 μg/mL in flasks and 380.0±166.2 μg/mL in bioreactors, **Table 1**). It should be noted that significant differences in the measured HCP concentration have previously been reported when using different ELISA assay kits. Specifically, when we measured the concentration of HCP in bioreactor supernatant samples using the Cygnus kit, the values were approximately 2.6 times lower than those determined with the Lonza GS-HCP kit [31]. Similar discrepancies were observed by Yuk et al. when comparing their results obtained with a proprietary Genentech HCP ELISA kit with those obtained by Tait et al. using the Cygnus kit [32,33] The specificity and accuracy thus appear to be different for each kit, hence, only the results obtained with the Lonza GS-HCP kit are presented here for consistency.

The extracellular HCP profile has been previously reported to be closely related to cell viability of bioreactors for this cell line [13]. Therefore, we wanted to know if the same relationship could be found between the extracellular HCP profile and cell viability of flasks. We plotted the percentage of dead cells (1-cell viability) as line graphs and superimposed it on bar charts of HCP concentration across the cell culture period (Figure S7). Instead of a trend of extracellular HCP level that increases directly with the percentage of dead cells, the extracellular HCP concentration of shake flask cultures was often underestimated by cell viability. This

trend indicates that HCPs in the supernatant collected from flasks were not released during the culture operation itself. Instead, we suspect that high percentages of apoptotic but viable cells sampled from flasks were sheared and broken down during the centrifugation step, releasing the HCPs into the supernatant.

3.4 The characteristics of HCPs when culture viability dropped below 80%

Figure 4A and B shows the number of HCP species found in supernatant samples under the two cultivation temperatures when cell viability dropped below 80%. A pool of HCPs was commonly found in both flask and bioreactor scales. Nonetheless, supernatants of bioreactors contained approximately 4 and 8.5 times higher number of different HCP species at standard physiological temperature and under mild hypothermia, respectively, compared to the respective flask cultures. This observation indicates that HCP composition was significantly more diverse in bioreactors than in flasks despite the same culture temperature in each case. Most HCP species found in flasks were detected in bioreactors too, i.e., 73% at standard physiological temperature and 93% under mild hypothermia.

HCP species in supernatants were categorized into their subcellular locations as described in Section 2.7 and the number and profile of HCP species are illustrated in **Figure 5**. Although the number of HCP species in supernatants was reduced substantially by culturing cells in flasks instead of bioreactors (**Figure 4**), the profile of their subcellular location was unaffected by the culture method at standard physiological temperature. From **Figure 5**A, the extracellular HCP mix in flasks was made up of 68% intracellular HCPs, 20% naturally secreted proteins and 12% membrane proteins. This distribution is similar to the HCP profile of the corresponding bioreactor cultures (**Figure 5**A), which agrees with previous reports that the majority of HCPs in supernatants are intracellular [13,33]. Interestingly, TDS to 32°C on day 5 modified this profile. From **Figure 5**B, the supernatant from flask cultures grown under mild hypothermia contained significantly fewer intracellular HCP species than the corresponding bioreactors, leading to an HCP composition mainly made up of naturally secreted proteins (48%), followed by intracellular proteins (37%) and cell membrane protein (15%). This suggests that the two culture methods led to protein expression differences at the reduced temperature of 32°C.

Moving from flasks to bioreactors also affected how the variety of HCP species related to apoptotic cell density of the cultures. In our previous study, we observed that the variety of HCP species is directly proportional to apoptotic cell density. [13]. When cell cultures were performed under mild hypothermia suppression of apoptotic cell density throughout the culture period led to a 37% reduction in the number of extracellular HCP species detected in supernatants [13]. Nonetheless, apoptotic cell density and the size of extracellular HCP pool did not correlate well when the impact of scale-up was considered. Shake flask supernatant, which contained a higher percentage of apoptotic cells (**Figure 2**), contained a significantly lower number of HCP species under both culture temperatures, as mentioned above (**Figure 4**). For instance, the percentage of apoptotic cells and the apoptotic cell

density in the control experiment were 76.2 ± 5.7% and 71.9 ± 13.7% lower in bioreactors than in flasks at the point of 80% cell viability (**Table 1**). However, the number of HCP species was 4 times higher in bioreactors than in flasks (**Table 1**).

This observation could not be due to higher HCP concentration in bioreactors as the HCP ELISA tests revealed comparable HCP levels in all four samples (**Table 1**). Interestingly, the HCP/IgG_4 ratio, which is a better indicator of the relative protein quantity in trypsin digested samples for LC-MS/MS analysis, were also comparable in all cases (**Table 1**). Therefore, the larger HCP diversity in bioreactors at both culture temperatures could not be due to higher level of HCPs in the supernatant both absolutely and relatively. Instead, the lower level of apoptotic cells in bioreactors was unlikely to be a result of improvements in the overall cell health but due to a higher rate of apoptotic cells dying and lysing in the bioreactor environment compared to in flasks. Cells might have been broken down by shear from aeration and mechanical stirring in bioreactors as soon as they turned apoptotic, and, therefore, undetected by the NC-250. Lysed cells released large quantity of HCPs of various kinds, which were then detected by the LC-MS/MS analysis. This study shows that the correlation between apoptotic cell density and the size of HCP composition of supernatants that we have previously reported for bioreactor studies is valid only when the same culture method is employed and that monitoring apoptotic cell density rather than culture viability is a better indicator of HCP diversity. This is in line with previous work by Yuk et al., who although Yuk et al., who confirmed that HCP composition does not change dramatically upon viability decline [32]. Our results further demonstrate that scale-up and culture method affect cell physiology and the resulting data significantly.

4 Conclusions

This study investigated how progressing cell cultures from shake flasks to bioreactors affects cellular behavior and consequently the profile of HCP in the culture supernatant under standard physiological temperature and with a shift to mild hypothermia in the exponential cell growth phase. We detected significant differences in cellular behavior between the two culture methods, which subsequently modified the extracellular profiles of HCP species, a major impurity in antibody preparations. Differences in cell growth and culture viability were particularly pronounced at standard physiological temperature, at which bioreactor cultures had significantly lower viability than flasks as early as day 10 of culture. We attributed this early cell death to hydrodynamic forces around the blade area, which have been previously documented for the particular disposable bioreactor used in this work. Under both temperatures, supernatant samples from bioreactor cultures were significantly richer in terms of variety of HCP species present, despite similar overall HCP concentration. Although the intracellular origin of these species was mostly preserved across flasks and bioreactors at physiological temperature, we observed significant discrepancies in HCP subcellular location between flask and bioreactor data for mild hypothermic cultures. Interestingly, the previously reported correlation between the number of HCP species in the supernatant and

apoptotic cell density observed for bioreactor cultures was not upheld in flask data, possibly because of the milder, lower shear environment. Importantly, our findings highlight the role of culture method and temperature on the variety of HCP species in the supernatant, which represents a potential burden on downstream separation units.

Acknowledgement

CHG and CK would like to thank Karen Polizzi for her advice on HCP categorization. CHG would like to thank the Department of Chemical Engineering, Imperial College London for her PhD scholarship.

Conflict of interest

The authors declare no financial or commercial conflict of interest.

5 References

1. Chon, J. H.; Zarbis-Papastoitsis, G. Advances in the production and downstream processing of antibodies. *N. Biotechnol.* **2011**, *28*, 458–463.
2. Hogwood, C. E. M.; Tait, A. S.; Koloteva-Levine, N.; Bracewell, D. G.; Smales, C. M. The dynamics of the CHO host cell protein profile during clarification and protein A capture in a platform antibody purification process. *Biotechnol Bioeng* **2013**, *110*, 240–251.
3. Doneanu, C.; Xenopoulos, A.; Fadgen, K.; Murphy, J.; Skilton, S. J.; Prentice, H.; Stapels, M.; Chen, W. Analysis of host-cell proteins in biotherapeutic proteins by comprehensive online two-dimensional liquid chromatography/mass spectrometry. *MAbs* **2012**, *4*, 24–44.
4. Levy, N. E.; Valente, K. N.; Choe, L. H.; Lee, K. H.; Lenhoff, A. M. Identification and characterization of host cell protein product-associated impurities in monoclonal antibody bioprocessing. *Biotechnol Bioeng* **2014**, *111*, 904–912.
5. Aboulaich, N.; Chung, W. K.; Thompson, J. H.; Larkin, C.; Robbins, D.; Zhu, M. A novel approach to monitor clearance of host cell proteins associated with monoclonal antibodies. *Biotechnol Progr* **2014**, *30*, 1114–1124.
6. Zhang, Q.; Goetze, A. M.; Cui, H.; Wylie, J.; Trimble, S.; Hewig, A.; Flynn, G. C. Comprehensive tracking of host cell proteins during monoclonal antibody purifications using mass spectrometry. *MAbs* **2014**, *6*, 659–670.
7. Chiverton, L. M.; Evans, C.; Pandhal, J.; Landels, A. R.; Rees, B. J.; Levison, P. R.; Wright, P. C.; Smales, C. M. Quantitative definition and monitoring of the host cell protein proteome using iTRAQ - a study of an industrial mAb producing CHO-S cell line. *Biotechnol J* **2016**, *11*, 1014–1024.
8. Bee, J. S.; Tie, L.; Johnson, D.; Dimitrova, M. N.; Jusino, K. C.; Afdahl, C. D. Trace levels of the CHO host cell protease cathepsin D caused particle formation in a monoclonal antibody product. *Biotechnol Progr* **2015**, *31*, 1360–1369.
9. Gao, S. X.; Zhang, Y.; Stansberry-Perkins, K.; Buko, A.; Bai, S.; Nguyen, V.; Brader, M. L. Fragmentation of a highly purified monoclonal antibody attributed to residual CHO cell protease activity. *Biotechnol Bioeng* **2011**, *108*, 977–982.
10. Chi, E. Y.; Krishnan, S.; Randolph, T. W.; Carpenter, J. F. Physical stability of proteins in aqueous solution: mechanism and driving forces in nonnative protein aggregation. *Pharm Res* **2003**, *20*, 1325–1336.
11. Valente, K. N.; Lenhoff, A. M.; Lee, K. H. Expression of difficult-to-remove host cell protein impurities during extended Chinese hamster ovary cell culture and their impact on continuous bioprocessing. *Biotechnol Bioeng* **2015**, *112*, 1232–1242.
12. Tait, A. S.; Tarrant, R. D. R.; Velez-Suberbie, M. L.; Spencer, D. I. R.; Bracewell, D. G. Differential response in downstream processing of CHO cells grown under mild hypothermic conditions. *Biotechnol Progr* **2013**, *29*, 688–696.
13. Goey, C. H.; Tsang, J. M. H.; Bell, D.; Kontoravdi, C. Cascading effect in bioprocessing - The impact of mild hypothermia on CHO cell behaviour and host cell protein composition. *Biotechnol Bioeng* **2017**, *114*, 2771–2781.
14. Park, J. H.; Jin, J. H.; Ji, I. J.; An, H. J.; Kim, J. W.; Lee, G. M. Proteomic analysis of host cell protein dynamics in the supernatant of Fc-fusion protein-producing CHO DG44 and DUKX-B11 cell lines in batch and fed-batch cultures. *Biotechnol Bioeng* **2017**, *114*, 2267–2278.

15. Jin, M.; Szapiel, N.; Zhang, J.; Hickey, J.; Ghose, S. Profiling of host cell proteins by two-dimensional difference gel electrophoresis (2D-DIGE): Implications for downstream process development. *Biotechnol Bioeng* **2010**, *105*, 306–316.
16. Kumar, N.; Gammell, P.; Meleady, P.; Henry, M.; Clynes, M. Differential protein expression following low temperature culture of suspension CHO-K1 cells. *BMC Biotechnol* **2008**, *8*, 1–13.
17. Al-Fageeh, M. B.; Marchant, R. J.; Carden, M. J.; Smales, C. M. The cold-shock response in cultured mammalian cells: Harnessing the response for the improvement of recombinant protein production. *Biotechnol Bioeng* **2006**, *93*, 829–835.
18. Farrell, A.; Mittermayr, S.; Morrissey, B.; Loughlin, N. M.; Iglesias, N. N.; Marison, I. W.; Bones, J. Quantitative host cell protein analysis using two dimensional data independent LC–MS^{E}. *Anal. Chem.* **2015**, *87*, 9186–9193.
19. Fan, Y.; del Val, I. J.; Müller, C.; Lund, A. M.; Sen, J. W.; Rasmussen, S. K.; Kontoravdi, C.; Baycin-Hizal, D.; Betenbaugh, M. J.; Weilguny, D.; Andersen, M. R. A multi-pronged investigation into the effect of glucose starvation and culture duration on fed-batch CHO cell culture. *Biotechnol Bioeng* **2015**, *112*, 2172–2184.
20. Kyriakopoulos, S.; Kontoravdi, C. A framework for the systematic design of fed-batch strategies in mammalian cell culture. *Biotechnol Bioeng* **2014**, *111*, 2466–2476.
21. Zhu, M. M.; Goyal, A.; Rank, D. L.; Gupta, S. K.; Vanden Boom, T.; Lee, S. S. Effects of elevated pCO_2 and osmolality on growth of CHO cells and production of antibody-fusion protein B1: a case study. *Biotechnol Progr* **2005**, *21*, 70–77.
22. Odeleye, A.; Marsh, D.; Osborne, M. D.; Lye, G. J. On the fluid dynamics of a laboratory scale single-use stirred bioreactor. *Chemical Engineering Science* **2014**.
23. Godoy-Silva, R.; Chalmers, J. J.; Casnocha, S. A.; Bass, L. A.; Ma, N. N. Physiological responses of CHO cells to repetitive hydrodynamic stress. *Biotechnol Bioeng* **2009**, *103*, 1103–1117.
24. Velez-Suberbie, M. L.; Tarrant, R. D. R.; Tait, A. S.; Spencer, D. I. R.; Bracewell, D. G. Impact of aeration strategy on CHO cell performance during antibody production. *Biotechnol Progr* **2013**, *29*, 116–126.
25. Clincke, M.-F.; Guedon, E.; Yen, F. T.; Ogier, V.; Roitel, O.; Goergen, J.-L. Effect of surfactant pluronic F-68 on CHO cell growth, metabolism, production, and glycosylation of human recombinant IFN-γ in mild operating conditions. *Biotechnol Progr* **2011**, *27*, 181–190.
26. Zhang, Z.; Al-Rubeai, M.; Thomas, C. R. Effect of Pluronic F-68 on the mechanical properties of mammalian cells. *Enzyme Microb. Technol.* **1992**, *14*, 980–983.
27. Roobol, A.; Roobol, J.; Carden, M. J.; Bastide, A.; Willis, A. E.; Dunn, W. B.; Goodacre, R.; Smales, C. M. ATR (ataxia telangiectasia mutated- and Rad3-related kinase) is activated by mild hypothermia in mammalian cells and subsequently activates p53. *Biochem J* **2011**, *435*, 499–508.
28. Al-Rubeai, M.; Singh, R. P.; Goldman, M. H.; Emery, A. N. Death mechanisms of animal cells in conditions of intensive agitation. *Biotechnol Bioeng* **1995**, *45*, 463–472.
29. Gorczyca, W.; Bruno, S.; Darzynkiewicz, R. J. DNA strand breaks occurring during apoptosis: Their early in situ detection by the terminal deoxynucleotidyl transferase

and nick translation assays and prevention by serine protease inhibitors. *Int J Oncol* **1992**, *1*, 639–648.
30. Motobu, M.; Wang, P. C.; Matsumura, M. Effect of shear stress on recombinant Chinese hamster ovary cells. *J. Ferment. Bioeng.* **1998**, *85*, 190–195.
31. Goey, C. H.; Bell, D.; Kontoravdi, C. Mild hypothermic culture conditions affect residual host cell protein composition post-Protein A chromatography. *MAbs* **2018**, 1–12.
32. Yuk, I. H.; Nishihara, J.; Walker, D.; Huang, E.; Gunawan, F.; Subramanian, J.; Pynn, A. F. J.; Yu, X. C.; Zhu-Shimoni, J.; Vanderlaan, M.; Krawitz, D. C. More similar than different: Host cell protein production using three null CHO cell lines. *Biotechnol Bioeng* **2015**, *112*, 2068–2083.
33. Tait, A. S.; Hogwood, C. E. M.; Smales, C. M.; Bracewell, D. G. Host cell protein dynamics in the supernatant of a mAb producing CHO cell line. *Biotechnol Bioeng* **2011**, *109*, 971–982.

Table 1. Performance indicators of cell culture when culture viability dropped below 80%.

Performance indicators	Control		32°C from day 5	
	Flasks	Bioreactors	Flasks	Bioreactors
Harvest day	15	9 and 11	17	14 and 16
Culture viability at harvest	79.5 ± 7.7	71.1 ± 7.3	79.9 ± 4.6	77.5 ± 2.1
IVCC (10^8 cells.h/mL)	20.1 ± 1.9	17.7 ± 4.7	21.6 ± 0.5	17.43 ± 2.1
Apoptotic cell (%)	8.4 ± 0.3	2.0 ± 0.3	5.5 ± 0.5	1.3 ± 0.2
Apoptotic cell density (10^5 cells/mL)	6.75 ± 0.54	1.90 ± 0.64	2.55 ± 0.38	0.71 ± 0.14
Specific antibody productivity[a] (pg/cell/day)	14.7 ± 1.0	16.1 ± 4.5	13.1 ± 1.1	15.3 ± 3.8
IgG4 titer (mg/mL)	1.23 ± 0.09	1.08 ± 0.15	0.85 ± 0.01	1.21 ± 0.15
HCP level (µg/mL)	330.9 ± 62.9	355.8 ± 132.9	272.0 ± 75.3	380.0 ± 166.2
HCP/IgG_4 (mg/mg)	0.27 ± 0.05	0.33 ± 0.13	0.32 ± 0.09	0.31 ± 0.14
HCP species (#)	88	363	27	231

a) Specific cell productivity is the average value from day 1 up to the harvest day.

Figure legends

Figure 1. Cell growth and cell viability of flasks and bioreactors at **A** standard physiological temperature (37°C in flasks and 36.5°C in bioreactors) or **B** with temperature downshift (TDS) to mild hypothermia (32°C) from day 5. Error bars are standard deviations of triplicate flask cultures and duplicate bioreactor runs. VCD, viable cell density

Figure 2. Cellular behavior: **A** Percentage of cells in apoptosis and **B** Percentage of cells in G_0/G_1 phase at standard physiological temperature (37°C in flasks and 36.5°C in bioreactors). Figures **C** and **D** show that of cell cultures under mild hypothermic conditions (32 °C from day 5). Error bars are standard deviations of triplicate flask cultures and duplicate bioreactor runs.

Figure 3. Product and impurity concentrations: **A** IgG_4 titer and **B** HCP level at standard physiological temperature (37°C in flasks and 36.5°C in bioreactors). Figures **C** and **D** show that of cell cultures under mild hypothermic conditions (32 °C from day 5). Error bars are standard deviations of triplicate flask cultures and duplicate bioreactor runs.

Figure 4. Variation in HCP species when cell viability dropped below 80%: Venn diagrams illustrate the number of HCP species found in flasks and bioreactors at **A** standard physiological temperature and **B** under mild hypothermia

Figure 5. Bar charts show the subcellular location of HCP species found in the HCCF at **A** standard physiological temperature and **B** under mild hypothermia. Pie charts show the proportion of HCP species in each subcellular location in bioreactors on the left and flasks on the right

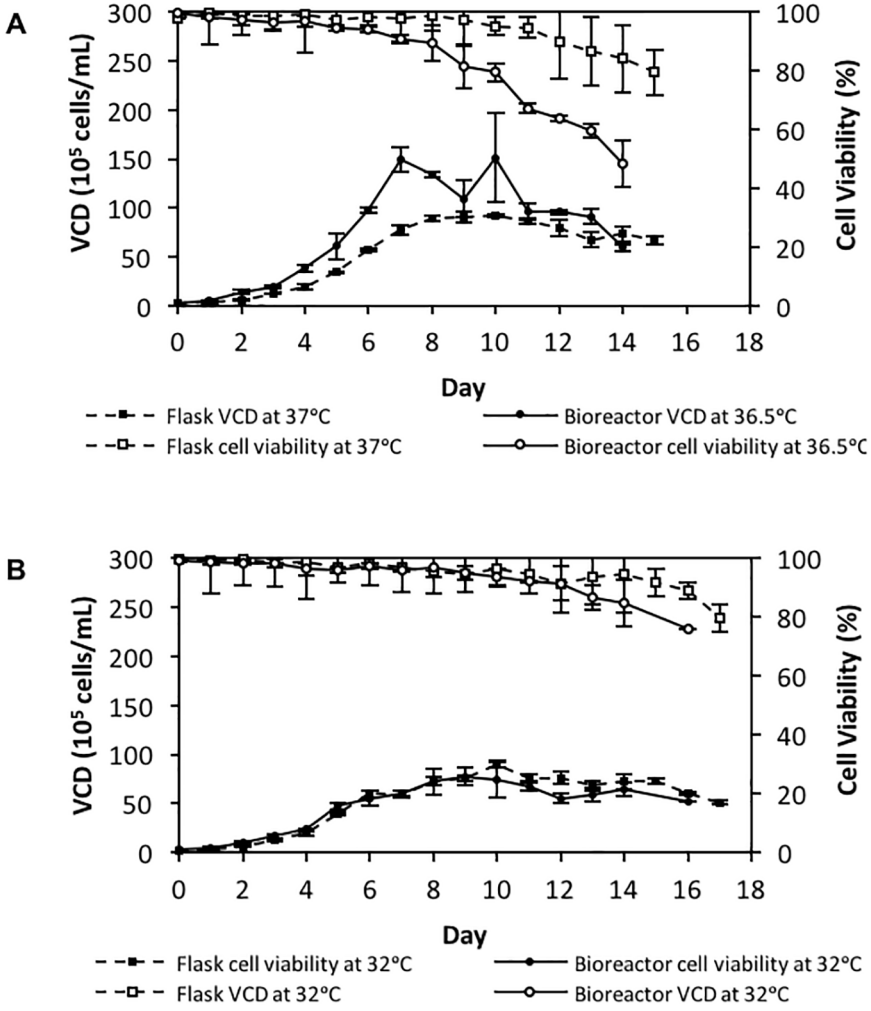

Figure 1. Cell growth and cell viability of flasks and bioreactors at **A** standard physiological temperature (37°C in flasks and 36.5°C in bioreactors) or **B** with temperature downshift (TDS) to mild hypothermia (32°C) from day 5. Error bars are standard deviations of flask triplicate and bioreactor duplicate. VCD, viable cell density

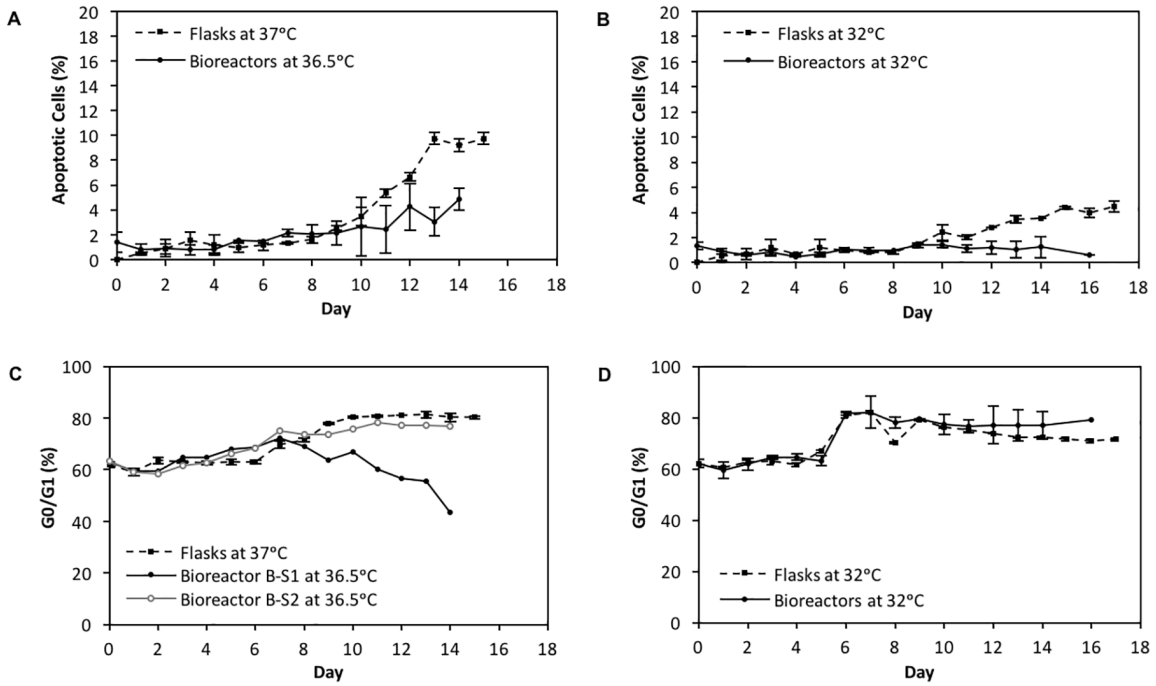

Figure 2. Cellular behavior: **A** Percentage of cells in apoptosis and **B** Percentage of cells in G_0/G_1 phase at standard physiological temperature (37°C in flasks and 36.5°C in bioreactors). Figures **C** and **D** show that of cell cultures under mild hypothermic conditions (32 °C from day 5). Error bars are standard deviations of flask triplicate and bioreactor duplicate

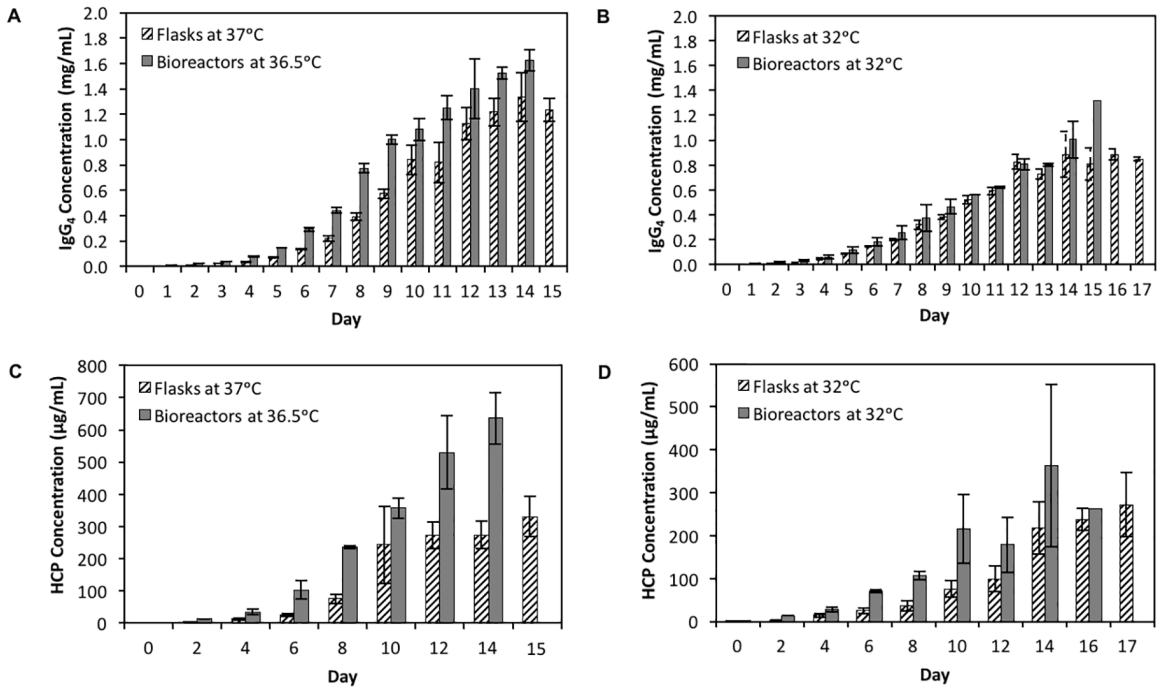

Figure 3. Product and impurity concentrations: **A** IgG_4 titer and **B** HCP level at standard physiological temperature (37°C in flasks and 36.5°C in bioreactors). Figures **C** and **D** show that of cell cultures under mild hypothermic conditions (32 °C from day 5). Error bars are standard deviations of flask triplicate and bioreactor duplicate

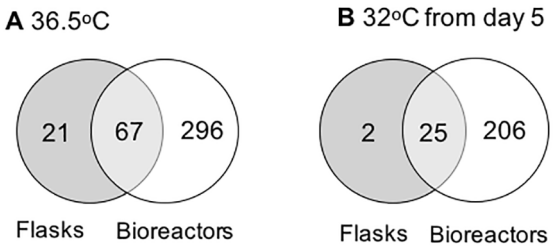

Figure 4. Variation in HCP species when cell viability dropped below 80%: Venn diagrams illustrate the number of HCP species found in flasks and bioreactors at **A** standard physiological temperature and **B** under mild hypothermia

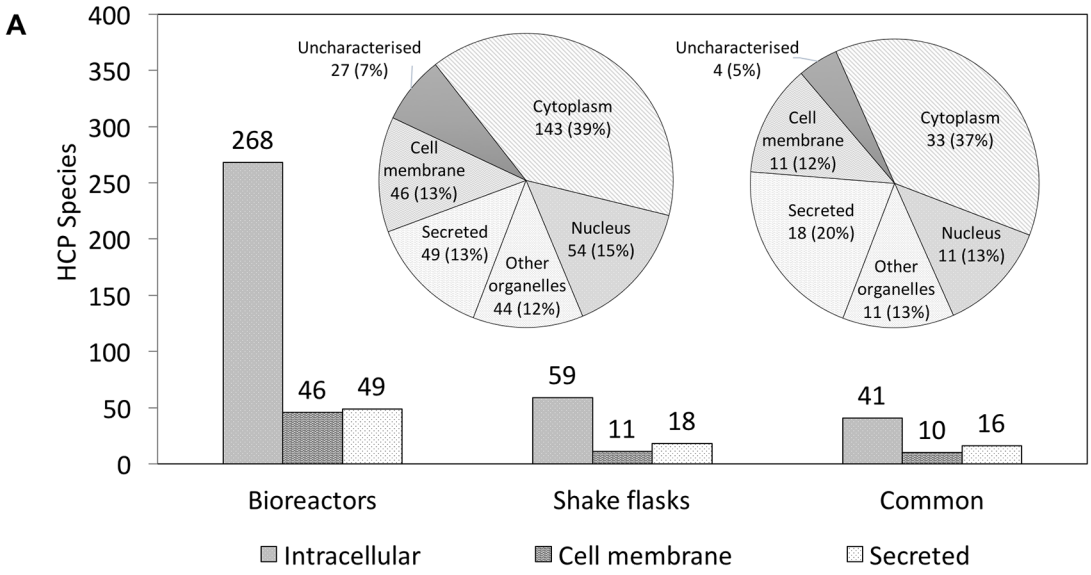

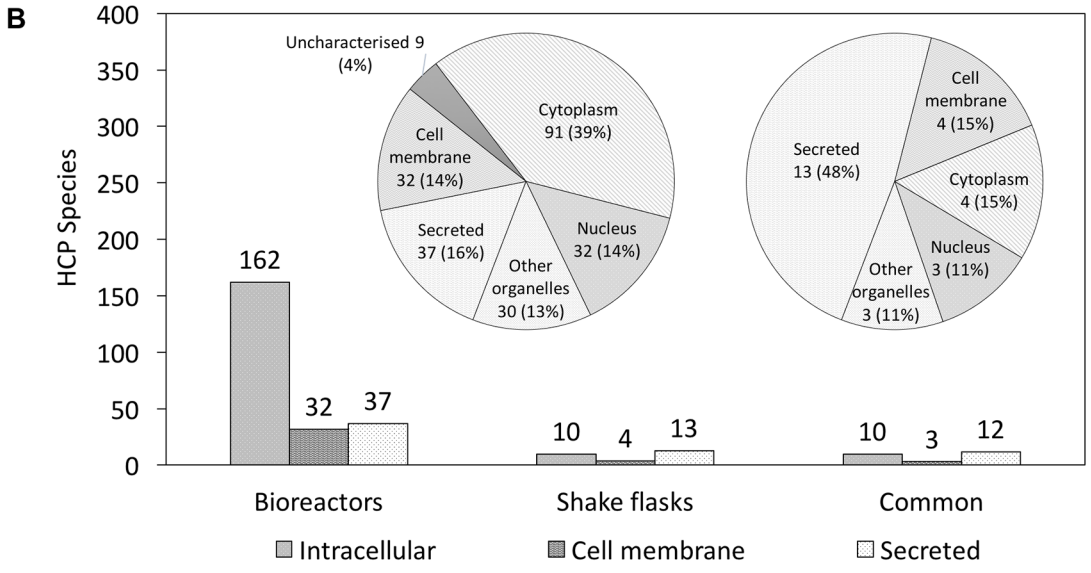

Figure 5. Bar charts show the subcellular location of HCP species found in the HCCF at **A** standard physiological temperature and **B** under mild hypothermia. Pie charts show the proportion of HCP species in each subcellular location in bioreactors on the left and flasks on the right